Coverage Optimisation for Aerial Wireless Networks

Shadi Eltanani
Faculty of Computing, Engineering and Sciences
Staffordshire University
Stoke-on-Trent, United Kingdom
e028131c@student.staffs.ac.uk

Ibrahim Ghafir
Department of Computer Science
University of Bradford
Bradford, United Kingdom
i.ghafir@bradford.ac.uk

***Abstract*—Unmanned Aerial Vehicles (UAVs) are considered, nowadays, as a futuristic and robust paradigm for 5G wireless networks, in terms of providing Internet connectivity services onto infrastructure cellular networks. In this paper, the interference regime caused by multiple downlink aerial wireless transmission beams has been highlighted. This has been introduced by estimating the UAVs coverage area that is analytically derived in a tractable closed-form expression. The rationale of the analysed coverage approach relies on observing and adapting the joint aerial distance between the aerial base stations. This can minimize the intra-overlapped coverage and ultimately maximize the overall coverage performance for a better quality of service demands. The novelty of our approach brings useful design insights for UAVs system-level performance that technically helps in aerial coverage computations without the need of performing an aerial deployment setup. To the end, the performance effectiveness of our methodology has been tested under an urban propagation environment conditions, in which the original probabilistic channel model approximation has been taken into account. Moreover, this paper identifies the interference issue of such an aerial network as a shrinkage or distortion phenomenon.**

***Index Terms*—Unmanned Aerial Vehicles (UAVs), 5G wireless Networks, Coverage Optimisation, Joint Aerial Distance, Interference, Quality of Service, Coverage Area.**

I. Introduction

Unmanned Aerial Vehicles (UAVs), commercially known as Drones, are considered as a key enabling technology for 5G wireless systems due to their robust effectiveness in boosting and leveraging wireless connectivity in the most severe hard-to-reach situations. UAVs can be used as flyable base station antennas that can be mounted on the drone itself due to their small size and light-weight [1]. Therefore, they have the ability to transmit their low-power capacity and to provide a visible line-of-sight (LoS) coverage range in either a downlink or an uplink direction accordingly. Unlike conventional communications which are prone to multipath and signal attenuation in various propagation environments, UAV communications are inevitably guaranteed due to the availability of line-of-sight (LoS) links. However, there are many inherited design issues with the aerial communication link between a single UAV itself and the connected destination point in such a direction. This is due to the adaptive propagation environment conditions that cause a severe deficiency on the reliability of aerial connectivity. Therefore, there is a necessity for key tractable procedures and methodologies that flexibly enhance and leverage efficient UAVs coverage deployment for different optimization purposes. This is aimed to wirelessly-yet-aerially manage and mitigate the problematic issue of interference.

It is worth mentioning that the main technical aerial communication challenges are basically presented in its performance analysis, channel modeling, optimal deployment, resource management, and energy efficiency [2, 3]. The majority of UAV communications research work has been targeted towards air-to-ground channel modeling [4, 5]. In this regard, the authors of [2] and [4] have empirically adopted the probabilistic line-of-sight (LoS) channel modeling for the air-to-ground communication as a function of the average height of building in such a dense urban propagation environment. This aerial channel modeling has been extensively used for most of the existing work [5, 6], where their channel characteristics are rely merely on the height of the aerial base station as specifically reported in [5].

To address the UAVs technical deployment of wireless connectivity challenges, the authors of [7] provided a simulation-based study of an optimal aerial placement for such a public safety communications use-case to enhance their coverage performance. The work of [8], on the other hand, introduced a generic practical overview of the integrating-use of UAVs with the cellular infrastructure network. However, the authors of [8] have not provided analytical coverage performance. Additionally, in [9], the integration use of UAVs with an infrastructure network has exploited for cell congestion overload and connectivity outage scenarios. In [10], the optimal location of UAVs has investigated in detail in order to enhance connectivity for an ad-hoc network, presuming that the aerial base stations have a pre-knowledge of their network users. Moreover, the authors of [3] reported the case of energy efficient and cell association deployment for multiple UAVs in a downlink direction.

For scenarios in which the coverage optimisation and

resource allocations of infrastructure cellular networks are prioritized, the need for considering interference management mitigation still remains crucial. The optimal altitude that a single static UAV can have and lead to a maximum coverage radius has been engineered in [4]. However, the trend of [4] has been implicitly introduced without a closed-form analytical formula, and it is dedicated for a deterministic coverage for an exempt-interference scenario case, in terms of comparing the average aerial path loss with a certain threshold. On the other hand, in [11] the authors have adopted the aerial interference issue. This was maintained by the case of deploying both multiple static UAVs where the optimal altitude and avoid-to-interference distance at a minimum transmit power have been claimed. The findings in [11] of estimating the UAVs coverage, however, are only simulations-based. Moreover, the overall coverage framework is still formulated in terms of multi-fold integrals, which do not provide direct insights on the impact of UAVs key system parameters such as the aerial link blockage, deploying at different altitudes, the separation distance, and so many others. However, the work introduced in [11] brings to the light the need for a more realistic yet tractable and analytical coverage area closed-form formula that can technically help engineers in optimising the aerial coverage area computations and without the need for performing an aerial real-deployment-setups.

The main contribution of this paper is fundamentally providing a comprehensive analysis and computations of the aerial coverage area for modeling and evaluation optimisations enhancement for next-generation wireless networks deployment design.

To reach our proposed solution, the closed-form analytical formula for aerial coverage radius that overseen in [4] in case of a single static UAV cell has been presented. Notably, the mathematically-proven tractable closed-form expression for UAVs coverage is verified with the aid of such an approximation-case to the original probabilistic channel model. The tuned approximated case probability is validated by simulation under a certain condition to be flexible enough to provide a line-of-sight coverage. This approximation case, however helps in estimating the aerial coverage that provides an agreement and close matching with original true simulation accordingly.

The proposed approach accounts for several important aspects that are overlooked in the previous work of [11], and most importantly it provides a direct insight on the impact of UAVs key system parameters for such interference case. It is worth noting that the aerial avoid-to-detect distance depends merely on how the UAVs coverage beam spot get shrunk in accordance with the allowable coverage radius. Therefore, a novel approach, in this paper, has been introduced, as an introductory-concept for investigating the effect of interference phenomenon on an aerial coverage area. This new approach is named as **SH**rinkage **A**rea **D**eformation **I**ndex (**SHADI**) law.

The rest of this paper is organized as follows. In section II, the system model is described. In section III, the analytical computation for aerial coverage area is reported. In section IV, the simulation results are analyzed. And finally, some conclusions are drawn in section V.

II. System Model

In this section, the geometric coverage beam spot of a single static UAV system has been introduced. The overall aerial link budget coverage criteria between the aerial base station and on-ground user, in case of exempt-interference regime, has been introduced.

A. Aerial-to-Ground Link and Channel Modeling Analysis

Motivated by the research paper reported in [12], there have been three-state path loss channel models that are scientifically recognized and empirically derived. These are considered for Line-of-Sight (LoS), Non Line-of-Sight (NLoS), and Outage Link (OL) whose probability of occurrence is totally based on distance-dependent. However, these models cannot be compatible with the operating principle of air-to-ground communication channels due to their 3D dimensional space. Consider an arbitrary channel link of length d, i.e. the Euclidean distance from the UAV$_j$ transmitter to an on-ground U$_i$ terminal-end, then the on-ground user U$_i$ could claim an aerial coverage if it is located within the coverage beam of this link. The indices $\{i, j\} \in \{1, 2\}$. Due to the large-scale environmental conditions in terms of signal transmission attenuations and higher rates of blockage, each link can be obviously in two different modes. Assume m denotes the set of $\mathcal{M}$ modes, i.e. $\mathcal{M} \in \{\mathrm{LoS}, \mathrm{NLoS}\}$. Then, the probability of being in such mode $m \in \mathcal{M}$ is denoted by $p_m(.)$, which is represented as a function of Θ_c and of other propagation environment dependent-factors such as α and β. This means $\sum_{m\in\mathcal{M}} p_m(\Theta_c) = 1$ for every Θ_c. Two-mode link models, for instance, due to the presence of buildings and obstacles can either be in LoS or NLoS respectively. Technically speaking, every type of link has an independent probability of occurrence and also the associated channels have different environmental parameters [2]. However, the likelihood occurrence is depended on the exponential of the user's location. Despite the uniqueness from the terrestrial communications channel models, the fact in [4] is considered as the corresponding 3D aerial channel probabilistic model. As a mathematical illustration, $p_m(.)$ can be formulated as follows:

$$p_m(\Theta_c) = \frac{1}{1 + \alpha \exp[-\beta(\frac{180}{\pi}\Theta_c - \alpha)]} \tag{1}$$

where α and β are dimensionless physical quantities that rely on the nature of the propagation environment such as urban, suburban, high-rise urban, and dense urban. Θ_c is denoted as the elevation angle formed by the inclination of

the transmitted signal path along with the corresponding user's coverage radius range directed from the projection of UAV$_j$ on ground. It can be expressed in radians or degrees as a function of UAV$_j$ altitude h_i and coverage radius R_i where $i \in \{1, 2\}$ as follows:

$$\Theta_c = (\frac{180}{\pi}) \arctan(\frac{h_i}{R_i}) \tag{2}$$

In Figure 1, a single static UAV system is elevated up to a certain altitude so as to provide its coverage beam into an arbitrary user U$_i$. The coverage beam spot is defined from the UAV$_j$ projection into ground O_i and the location of targeted user U$_i$ accordingly. The horizontal distance R_i then identifies whether the aerial coverage has been fulfilled or not.

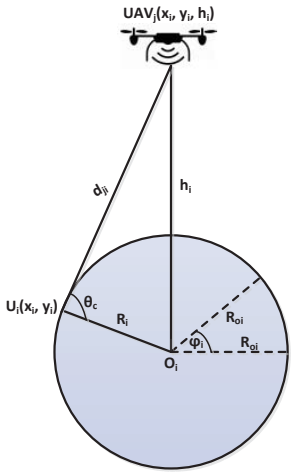

Fig. 1. A single UAV small cell coverage

In accordance to (1), the effect of free-space propagation path loss is considered for both link state modes, i.e. LoS and NLoS [4], respectively. By considering a link of length d in such a mode $m \in \mathcal{M}$, then the two-mode distance-dependent free-space path loss model in dB-scale can be denoted as $l_m(.)$ and expressed as follows:

$$\bigcup_{m \in \{\text{LoS}, \text{NLoS}\}, i \neq j} l_m(d_{ij}) = 20 \log_{10}(\kappa d_{ij}) + \chi_m \tag{3}$$

Where, $\kappa = \frac{4\pi f_c}{v_o}$ is the path loss constant as a function of the carrier frequency f_c and the physical speed of light v_o. The Euclidean distance d_{ji} is defined as the path loss distance from the UAV and receiving user-end on-ground, as shown in Figure 1. Using Pythagoras theorem, it can be mathematically notated as, $d_{ji} = \sqrt{R_i^2 + h_i^2}$, where the coverage radius R_i can be analytically defined as $R_i = \sqrt{(x_i - x_j)^2 + (y_i - y_j)^2}$. Also, χ_m accounts for the additional mean excessive path loss value that assigned to LoS and NLoS propagation links. In fact, this impact experiences less effect in LoS mode than the other mode of NLoS. However, the path loss in the NLoS propagation path is significantly larger than its counterpart of LoS mode, owing to the inherited variations of environmental shadowing behavior and reflected signals from various objects [13, 14].

The overall averaged aerial free-space probabilistic path loss model $l_m^T(.)$ can be formulated by the following notation as follows:

$$\overline{l_m^T(d_{ij})} = \{\frac{\chi_{LoS} - \chi_{NLoS}}{1 + \alpha \exp[-\beta(\frac{180}{\pi}\Theta_c - \alpha)]}\} + \digamma_1. \tag{4}$$

where, $\digamma_1 = \{20 \log_{10}(\kappa\sqrt{R_i^2 + h_i^2}) + \chi_{\text{NLoS}}\}$

In this paper, however, the fact of adopting an approximated-case, for the probabilistic channel model introduced in (1) for air-to-ground communications, is addressed by the authors. It has been used in our paper with the aid of **SHADI** law for the aerial coverage area computation which provides a significant agreement with the original case model. Basically, the original aerial channel model of (1) represents a binomial series with negative integer n= -1. This means that all of the terms in the series expression $n(n-1)(n-2)...$ will be negative and non of the terms will ever be zero, and hence the series will not terminate. Therefore, in order to have a finite sum for an infinite series it must be convergent and this reflects that all the series terms require to get smaller and smaller. This can be truly valid if $|1 + \alpha \exp[-\beta(\frac{180}{\pi}\Theta_c - \alpha)]| < 1$. However, the condition $|1 + \alpha \exp[-\beta(\frac{180}{\pi}\Theta_c - \alpha)]| < 1$ is invalid for our aerial coverage analysis as it eventually cannot guarantee the line-of-sight (LoS) status for an aerial link. Therefore, the equation of (1) has been tuned to a such approximation case to maintain the aerial system requirements in terms of ensuring that the average path loss is to be within a LoS and NLoS status modes. This approximated-case is set under certain conditions, e.g. $\widetilde{p}_m(\Theta_c) \approx \frac{1}{\alpha \exp[-\beta(\frac{180}{\pi}\Theta_c - \alpha)]}$ such that for the $\alpha \exp[-\beta(\frac{180}{\pi}\Theta_c - \alpha)] \gg 1$ the condition $R_{min} < R_{oi} < R_{max}$ is obeyed. The R_{oi} is the bounded coverage radius that maintains the aerial link in both LoS and NLOs modes. Then this approximated model describes a semi-linearly aerial propagation link between the UAV$_j$ system and the on-ground user U$_i$ with a monotonically increasing elevation angle Θ_c. As long as this remains a good approximation, it can perfectly describe the existence of LoS and NLoS status modes for all times. In this paper, this approximated property is being called the "clearance-aerial-link approximation"for aerial UAVs channel modeling.

The accuracy of the approximated-case probabilistic channel model has been validated by means of simulation against the true original model as shown in Figure 2. It is worth noting that, this approximated-case has been utilized in estimating the coverage area for multiple aerial systems. Fortunately enough, it introduces with the aid of **SHADI** law a significant agreement-and-matching with the original coverage area estimation. Further details are given in subsequent sections.

III. Coverage Area Estimation

In this section, the total aerial coverage area on the ground provided by multiple aerial transmission beam is derived.

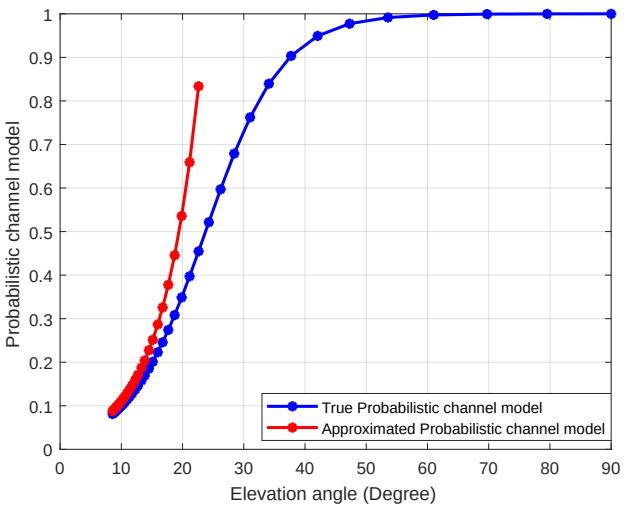

Fig. 2. Comparison between original and approximated probabilistic channel model

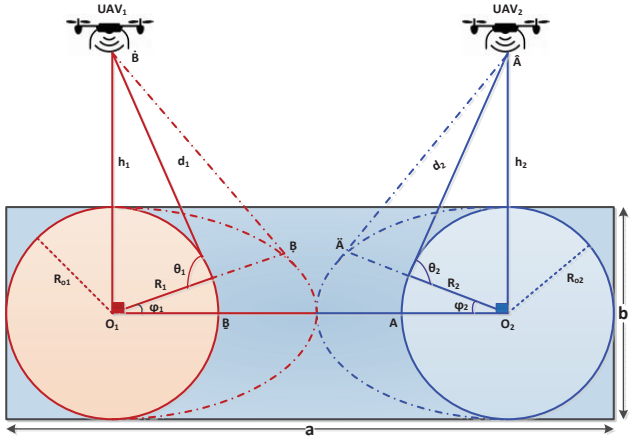

Fig. 3. Aerial coverage beam spots for multiple UAVs

Consider a pre-defined geographical rectangular area with geometric dimensions $a \times b \subset \mathbb{R}$, where a and b are the length in meters respective to the targeted area of interest dimensions. The ground users U_i are uniformly distributed in a lattice manner over the infrastructure cellular network. Figure 3 shows a scenario depicting an aerial cellular system where every single small cell is positioned at an altitude h_i. This aerial altitude forms an elevation angle Θ_{ci} with respect to the horizontal coverage radius along x-axis that determines the beam limit of covered users U_i on-ground. The index $i \in \{1, 2\}$. Assuming that the aerial transmitter UAV_j is settled at the center of its coverage beam, then the mathematical coverage representation can be given as:

$$UAV_j(O_i, R_i, D) = \left(O_i(x_i, y_i), \frac{h_i}{\tan(\Theta_c)}, D_o\right) \tag{5}$$

where, R_i is the allowable coverage radius, $O_i(x_i, y_i)$ is the projection of aerial base station onto 2D horizontal coverage space on the ground, $D = D_o$ is the UAV_j joint distance with respect to each other on the ground which needs to be balanced.

Without the loss of generality, one of the UAVs is deployed at a fixed projection, whereas the other is instantaneously deployed afterwards maintaining a complete coverage of the former aerial system. This is to monitor and calibrate the aerial joint distance with respect to each other accordingly. The former is positioned at $(\frac{a}{2} - \widehat{R}_{max2}, 0)$ and the latter at $(-\frac{a}{2} + \widehat{R}_{max1}, 0)$. The non-interfering maximal coverage radii associated with both UAV_j are denoted as $\widehat{R}_{max1}$ and $\widehat{R}_{max2}$ respectively. Also, these radii describe the characteristics of the coverage beam that extends from the origin of projection to cell boundary at scanning coverage angle φ_i. It is worth noting that the aerial coverage of non-overlapping radii experiences a significant morph change by a factor of $\epsilon_f R_i$ due to the variation of separation distance and spatio-temporal change of users U_i. The $\epsilon_f R_i$ can also interpret the change in coverage radius from O_2A to $A\ddot{A}$ and similarly from $O_1\underline{B}$ to $\underline{B}\dot{\mathrm{B}}$ as seen in Figure 4. As a result of that, the overall coverage get to expand and hence the edges of the targeted area gets to aerially be covered as well. To reflect on **SHADI** law, as both aerial systems try to get closer to or even move far away from each other, then the aerial coverage will shrink by a factor of ρ_f. The aerial distance proximity causes the beam spots of coverage area to shrink meaning that the average rate of SNR becomes weak and cannot fulfill the quality of service demands of users. Hence, the overall aerial coverage area can be presented as:

$$A_j = \left(\frac{1}{\rho_f}\right)\left\{\epsilon_f^2\left[R_i^2 + \left(\frac{b^2}{4}\right)\right]\Phi_o + \delta_o\Psi_o\right\} \tag{6}$$

where,

$$R_i \cong \sqrt[56]{\left\{\frac{|\Xi_1|}{|\Xi_2|}\right\}} \tag{7}$$

with,

$$\begin{aligned}\Xi_1 = (13440h_i^{14})([(\chi_{LoS} - \chi_{NLoS})(\alpha \mathrm{e}^{\alpha\beta})^{-1} \\ [738112500\beta^6 + 49207500\beta^5 + 2733750\beta^4 + 121500\beta^3 \\ + 4050\beta^2 + 90\beta + 1] + 20\log_{10}(\frac{4\pi f_c}{\upsilon_o}) + 20\log_{10} h_i \\ + \chi_{NLoS} + (P_{t,i} - \sigma^2 - \gamma)]).\end{aligned}$$

$$\Xi_2 = 105(\chi_{LoS} - \chi_{NLoS})(\alpha \mathrm{e}^{\alpha\beta})^{-1}\left(\frac{472392 \times 10^5\beta^6}{117649h^{42}\pi^6}\right).$$

$$\Phi_o = \arctan\left(\frac{b}{2R_i}\right).$$

$$\delta_o = \left[\sqrt{\left[D + \left(\epsilon_f\sqrt{R_i^2 + (\tfrac{b^2}{4})}\right) - a\right]^2 + (\tfrac{b^2}{4})}\right].$$

$$\Psi_o = \arctan\left[\frac{b}{2\left(D+\left(\epsilon_f\sqrt{R_i^2+(\frac{b^2}{4})}\right)-a\right)}\right].$$

IV. Simulation Results and Analysis

In this section, the analytical results of our derived aerial coverage area have been compared with the simulation results. The details of the simulation setup are provided in Table 1 shown below.

TABLE I
SIMULATION PARAMETERS

Simulation Parameters	Values
Propagation Environment	Urban
Carrier Frequency (f_c)	2 GHz
Transmission Power (P_t)	2 W
χ_{LoS}	1 dB
χ_{NLoS}	20 dB
Noise Power (σ^2)	-150 dBm
α [15]	9.61
β [15]	0.16
Targeted Area Dimensions ($a \times b$)	(2000×700) m^2
SNR threshold (γ)	10 dB

In Figure 4 and 5, the UAVs wireless optimum coverage is shown at various aerial altitudes of $100m$ and $200m$ respectively at which their optimal distances are observed at $1065m$ and $930m$ respectively. The enhanced-aerial coverage has been validated within a targeted area of 2000×700 dimensions. It is observed that due to the proximity of joint horizontal distance, then there is a shrinkage or distortion rate that occurred to the overall coverage area on the ground. This is due to the interference effect highlighted in **SHADI** law for aerial coverage. Figure 4 and 5 give also a physical meaning or a performance metric measure for wireless coverage on how to quantify an aerial coverage over a particular geographic area in order to balance the separation distance for maximal and enabling coverage challenge demands. In general, the avoid-to-interference distance depends on the aerial altitude. Hence, increasing the joint distance results in decreasing the coverage radius. Furthermore, at low altitude levels the coverage shrinkage becomes higher than that at high altitude level, e.g. $\rho_f(h = 200m) < \rho_f(h = 100m)$, as shown in Figure 4 and 5 accordingly.

Increasing the shrinkage rate is primarily due to the significant increase in the coverage radius. In other words, the more aerial altitude, the more observable coverage and less shrinkage rate due to the line-of-sight (LoS) dominance. Noticeably, the UAVs coverage beam spots shown in Figure 4 and 5 is being cut and, hence, fitted within the targeted area boundaries only. This coverage shape does look like Cassini-Oval curvature; the shape that represents the circulation of Sun around the Earth. In our paper, due to the boundaries of the targeted area of interest, the shape of the ground aerial coverage is being re-named to 'Rectangular-Compressed Cassini Ovals' (RCCOs) shape.

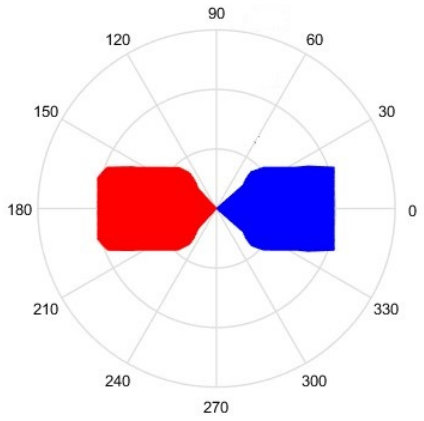

Fig. 4. UAVs optimal coverage at h= 100m

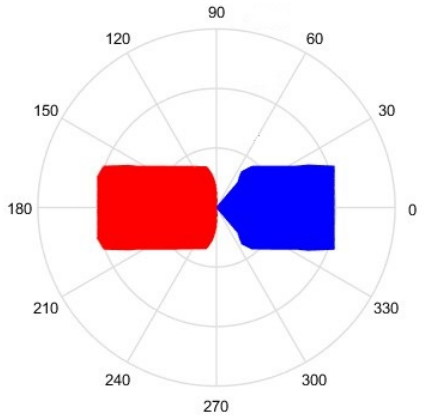

Fig. 5. UAVs optimal coverage at h= 200m

In Figure 6, the shrinkage coverage area index has been illustrated against the joint aerial distance at various altitudes. It interprets how much the aerial coverage area gets shrink in case of calibrating the distance among multiple aerial systems. It also spots the light on the scientific meaning of **SHADI** law for aerial coverage in terms of the inverse-proportional relationship between the shrinkage index rate and joint separation distance as well.

V. Conclusion

In this paper, the overall aerial coverage area for multiple UAV systems has been introduced, and its mathematical closed-form expression been analytically derived. The accuracy of the contributed derived aerial coverage area approach has been substantiated with the introduction-aid of **SHADI** law. This closed-form expression has a tremendous insight for UAV coverage area optimisation in different propagation

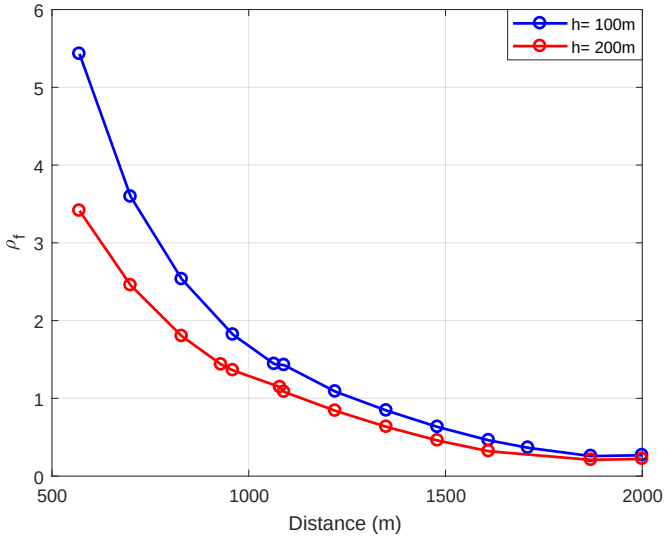

Fig. 6. Shrinkage rate index versus the aerial avoid-to-interference distance at various aerial altitudes

deployment environments, whereas it also provides several conclusions on the integrity of such aerial base stations in space safely that extensively help engineers in UAV systems design.

REFERENCES

[1] L. Afonso, N. Souto, P. Sebastiao, M. Ribeiro,T. Tavares, and R. Marinheiro, "Cellular for theskies: Exploiting mobile network infrastructure forlow altitude air-to-ground communications,"IEEEAerospace and Electronic Systems Magazine, vol. 31,no. 8, pp. 4–11, 2016.

[2] Q. Feng, E. K. Tameh, A. R. Nix, and J. McGeehan,"Wlcp2-06: modelling the likelihood of line-of-sightfor air-to-ground radio propagation in urban environ-ments," inGlobal Telecommunications Conference,2006. GLOBECOM'06. IEEE.IEEE, 2006, pp. 1–5.

[3] M. Mozaffari, W. Saad, M. Bennis, and M. Debbah,"Optimal transport theory for power-efficient deployment of unmanned aerial vehicles," inCommunica-tions (ICC), 2016 IEEE International Conference on.IEEE, 2016, pp. 1–6.

[4] A. Al-Hourani, S. Kandeepan, and S. Lardner, "Optimal lap altitude for maximum coverage,"IEEEWireless Communications Letters, vol. 3, no. 6, pp.569–572, 2014.

[5] J. Holis and P. Pechac, "Elevation dependent shad-owing model for mobile communications via highaltitude platforms in built-up areas,"IEEE Transac-tions on Antennas and Propagation, vol. 56, no. 4,pp. 1078–1084, 2008.

[6] Q. Feng, J. McGeehan, E. K. Tameh, and A. R. Nix,"Path loss models for air-to-ground radio channels inurban environments," inVehicular Technology Con-ference, 2006. VTC 2006-Spring. IEEE 63rd, vol. 6.IEEE, 2006, pp. 2901–2905.

[7] J. Kosmerl and A. Vilhar, "Base stations place-ment optimization in wireless networks for emer-gency communications," inCommunications Work-shops (ICC), 2014 IEEE International Conferenceon. IEEE, 2014, pp. 200–205.

[8] K. Daniel and C. Wietfeld, "Using public networkinfrastructures for uav remote sensing in civiliansecurity operations," Dortmund Univ (Germany FR),Tech. Rep., 2011.

[9] S. Rohde and C. Wietfeld, "Interference aware positioning of aerial relays for cell overload and outagecompensation," inVehicular Technology Conference(VTC Fall), 2012 IEEE. IEEE, 2012, pp. 1–5.

[10] Z. Han, A. L. Swindlehurst, and K. R. Liu, "Op-timization of manet connectivity via smart deploy-ment/movement of unmanned air vehicles,"IEEETransactions on Vehicular Technology, vol. 58, no. 7,pp. 3533–3546, 2009.

[11] M. Mozaffari, W. Saad, M. Bennis, and M. Debbah,"Drone small cells in the clouds: Design, deploymentand performance analysis," inGlobal Communica-tions Conference (GLOBECOM), 2015 IEEE. IEEE,2015, pp. 1–6.

[12] M. Di Renzo, "Stochastic geometry modeling andanalysis of multi-tier millimeter wave cellular networks,"IEEE Transactions on Wireless Communications, vol. 14, no. 9, pp. 5038–5057, 2015.

[13] M. Mozaffari, W. Saad, M. Bennis, and M. Debbah,"Unmanned aerial vehicle with underlaid device-to-device communications: Performance and tradeoffs,"IEEE Transactions on Wireless Communications,vol. 15, no. 6, pp. 3949–3963, 2016.

[14] H. Ghazzai, E. Yaacoub, M.-S. Alouini, Z. Dawy,and A. Abu-Dayya, "Optimized lte cell planning withvarying spatial and temporal user densities,"IEEETransactions on Vehicular Technology, vol. 65, no. 3,pp. 1575–1589, 2016.

[15] J. Lu, S. Wan, X. Chen, and P. Fan, "Energy-efficient3d uav-bs placement versus mobile users' densityand circuit power,"arXiv preprint arXiv:1705.06500,2017.